

31

Lumped and Consistent Mass Matrices

TABLE OF CONTENTS

	Page
§31.1. Introduction	31-3
§31.2. Mass Matrix Construction	31-3
§31.2.1. Direct Mass Lumping	31-3
§31.2.2. Variational Mass Lumping	31-4
§31.2.3. Template Mass Lumping	31-4
§31.2.4. Mass Matrix Properties	31-5
§31.2.5. Rank and Numerical Integration	31-6
§31.3. Globalization	31-6
§31.4. Mass Matrix Examples: Bars and Beams	31-8
§31.4.1. The 3-Node Bar	31-8
§31.4.2. The Bernoulli-Euler Plane Beam	31-8
§31.4.3. The Plane Beam-Column	31-10
§31.4.4. *The Timoshenko Plane Beam	31-11
§31.4.5. *Spar and Shaft Elements	31-12
§31.5. Mass Matrix Examples: Plane Stress	31-12
§31.5.1. The Plane Stress Linear Triangle	31-12
§31.5.2. Four-Node Bilinear Quadrilateral	31-14
§31.6. Mass Diagonalization Methods	31-15
§31.6.1. HRZ Lumping	31-15
§31.6.2. Lobatto Lumping	31-15
§31. Notes and Bibliography	31-16
§31. References	31-18
§31. Exercises	31-19

§31.1. Introduction

To do dynamic and vibration finite element analysis, you need at least a mass matrix to pair with the stiffness matrix. This Chapter provides a quick introduction to standard methods for computing this matrix.

As a general rule, the construction of the master mass matrix \mathbf{M} largely parallels that of the master stiffness matrix \mathbf{K} . Mass matrices for individual elements are formed in local coordinates, transformed to global, and merged into the master mass matrix following exactly the same techniques used for \mathbf{K} . In practical terms, the assemblers for \mathbf{K} and \mathbf{M} can be made identical. This procedural uniformity is one of the great assets of the Direct Stiffness Method.

A notable difference with the stiffness matrix is the possibility of using a *diagonal* mass matrix based on direct lumping. A master diagonal mass matrix can be stored simply as a vector. If all entries are nonnegative, it is easily inverted, since the inverse of a diagonal matrix is also diagonal. Obviously a lumped mass matrix entails significant computational advantages for calculations that involve \mathbf{M}^{-1} . This is balanced by some negative aspects that are examined in some detail later.

§31.2. Mass Matrix Construction

The master mass matrix is built up from element contributions, and we start at that level. The construction of the mass matrix of individual elements can be carried out through several methods. These can be categorized into three groups: direct mass lumping, variational mass lumping, and template mass lumping. The last group is more general in that it includes all others. Variants of the first two techniques are by now standard in the FEM literature, and implemented in all general purpose codes. Consequently this Chapter covers the most widely used methods, focusing on techniques that produce diagonally lumped and consistent mass matrices. The next Chapter covers the template approach to produce customized mass matrices.

§31.2.1. Direct Mass Lumping

The total mass of element e is directly apportioned to nodal freedoms, ignoring any cross coupling. The goal is to build a *diagonally lumped mass matrix* or DLMM, denoted here by \mathbf{M}_L^e .

As the simplest example, consider a 2-node prismatic bar element with length ℓ , cross section area A , and mass density ρ , which can only move in the axial direction x , as depicted in Figure 31.1. The total mass of the element is $M^e = \rho A \ell$. This is divided into two equal parts and assigned to each end node to produce

$$\mathbf{M}_L^e = \frac{1}{2} \rho A \ell \begin{bmatrix} 1 & 0 \\ 0 & 1 \end{bmatrix} = \frac{1}{2} \rho A \ell \mathbf{I}_2, \quad (31.1)$$

in which \mathbf{I}_2 denotes the 2×2 identity matrix. As shown in the figure, we have replaced the bar with a “dumbbell.”

This process conserves the translational kinetic energy or, equivalently, the linear momentum. To show this for the bar example, take the constant x -velocity vector $\dot{\mathbf{u}}^e = v [1 \ 1]^T$. The kinetic

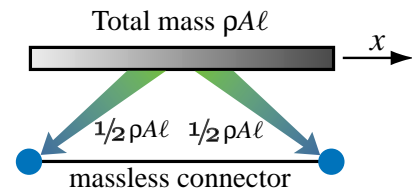


FIGURE 31.1. Direct mass lumping for 2-node prismatic bar element.

energy of the element is $T^e = \frac{1}{2}(\dot{\mathbf{u}}^e)^T \mathbf{M}_L^e \dot{\mathbf{u}}^e = \frac{1}{2}\rho A \ell v^2 = \frac{1}{2}M^e v^2$. Thus the linear momentum $p^e = \partial T^e / \partial v = M^e v$ is preserved. When applied to simple elements that can rotate, however, the direct lumping process may not necessarily preserve *angular* momentum.

A key motivation for direct lumping is that, as noted in §31.1, a diagonal mass matrix may offer computational and storage advantages in certain simulations, notably explicit time integration. Furthermore, direct lumping covers naturally the case where concentrated (point) masses are natural part of model building. For example, in aircraft engineering it is common to idealize nonstructural masses (fuel, cargo, engines, etc.) as concentrated at given locations.¹

§31.2.2. Variational Mass Lumping

A second class of mass matrix construction methods are based on a variational formulation. This is done by taking the *kinetic energy* as part of the governing functional. The kinetic energy of an element of mass density ρ that occupies the domain Ω^e and moves with velocity field $\vec{\mathbf{v}}^e$ is

$$T^e = \frac{1}{2} \int_{\Omega^e} \rho (\vec{\mathbf{v}}^e)^T \vec{\mathbf{v}}^e d\Omega^e. \quad (31.2)$$

Following the FEM philosophy, the element velocity field is interpolated by shape functions: $\vec{\mathbf{v}}^e = \mathbf{N}_v^e \dot{\mathbf{u}}^e$, where $\dot{\mathbf{u}}^e$ are node DOF velocities and \mathbf{N}_v^e a shape function matrix. Inserting into (31.2) and moving the node velocities out of the integral gives

$$T^e = \frac{1}{2}(\dot{\mathbf{u}}^e)^T \int_{\Omega^e} \rho (\mathbf{N}_v^e)^T \mathbf{N}_v^e d\Omega \dot{\mathbf{u}}^e \stackrel{\text{def}}{=} \frac{1}{2}(\dot{\mathbf{u}}^e)^T \mathbf{M}^e \dot{\mathbf{u}}^e, \quad (31.3)$$

whence the element mass matrix follows as the Hessian of T^e :

$$\mathbf{M}^e = \frac{\partial^2 T^e}{\partial \dot{\mathbf{u}}^e \partial \dot{\mathbf{u}}^e} = \int_{\Omega^e} \rho (\mathbf{N}_v^e)^T \mathbf{N}_v^e d\Omega. \quad (31.4)$$

If the same shape functions used in the derivation of the stiffness matrix are chosen, that is, $\mathbf{N}_v^e = \mathbf{N}^e$, (31.4) is called the *consistent mass matrix*² or CMM. It is denoted here by \mathbf{M}_C^e .

For the 2-node prismatic bar element moving along x , the stiffness shape functions of Chapter 12 are $N_i = 1 - (x-x_i)/\ell = 1 - \zeta$ and $N_j = (x-x_i)/\ell = \zeta$. With $dx = \ell d\zeta$, the consistent mass is easily obtained as

$$\mathbf{M}_C^e = \int_0^\ell \rho A (\mathbf{N}^e)^T \mathbf{N}^e dx = \rho A \int_0^1 \begin{bmatrix} 1 - \zeta \\ \zeta \end{bmatrix} [1 - \zeta \quad \zeta] \ell d\zeta = \frac{1}{6}\rho A \ell \begin{bmatrix} 2 & 1 \\ 1 & 2 \end{bmatrix}. \quad (31.5)$$

It can be verified that this mass matrix preserves linear momentum along x .

¹ Such concentrated masses in general have rotational freedoms. Rotational inertia lumping is then part of the process.

² A better name would be stiffness-consistent. The shorter sobriquet has the unfortunately implication that other choices are “inconsistent,” which is far from the truth. In fact, the consistent mass is not necessarily the best one, a topic elaborated in the next Chapter. However the name is by now ingrained in the FEM literature.

§31.2.3. Template Mass Lumping

A generalization of the two foregoing methods consists of expressing the mass as a linear combination of k component mass matrices:

$$\mathbf{M}^e = \sum_{i=1}^k \mu_i \mathbf{M}_i^e. \quad (31.6)$$

Appropriate constraints on the free parameters μ_i are placed to enforce matrix properties discussed in §31.2.4. Variants result according to how the component matrices \mathbf{M}_i are chosen, and how the parameters μ_i are determined. The best known scheme of this nature results on taking a weighted average of the consistent and diagonally-lumped mass matrices:

$$\mathbf{M}_{LC}^e \stackrel{\text{def}}{=} (1 - \mu) \mathbf{M}_C^e + \mu \mathbf{M}_L^e, \quad (31.7)$$

in which μ is a free scalar parameter. This is called the LC (“lumped-consistent”) weighted mass matrix. If $\mu = 0$ and $\mu = 1$ this combination reduces to the consistent and lumped mass matrix, respectively. For the 2-node prismatic bar we get

$$\mathbf{M}_{LC}^e = (1 - \mu) \frac{1}{6} \rho A \ell \begin{bmatrix} 2 & 1 \\ 1 & 2 \end{bmatrix} + \mu \frac{1}{2} \rho A \ell \begin{bmatrix} 1 & 0 \\ 0 & 1 \end{bmatrix} = \frac{1}{6} \rho A \ell \begin{bmatrix} 2 + \mu & 1 - \mu \\ 1 - \mu & 2 + \mu \end{bmatrix}. \quad (31.8)$$

It is known (since the early 1970s) that the best choice with respect to minimizing low frequency dispersion is $\mu = 1/2$. This is proven in the next Chapter.

The most general method of this class uses *finite element templates* to fully parametrize the element mass matrix. For the prismatic 2-node bar element one would start with the 3-parameter template

$$\mathbf{M}^e = \rho A \ell \begin{bmatrix} \mu_{11} & \mu_{12} \\ \mu_{12} & \mu_{22} \end{bmatrix}, \quad (31.9)$$

which includes the symmetry constraint from the start. Invariance requires $\mu_{22} = \mu_{11}$, which cuts the free parameters to two. Conservation of linear momentum requires $\mu_{11} + \mu_{12} + \mu_{12} + \mu_{22} = 2\mu_{11} + 2\mu_{12} = 1$, or $\mu_{12} = 1/2 - \mu_{11}$. Taking $\mu = 6\mu_{11} - 2$ reduces (31.9) to (31.8). Consequently for the 2-node bar LC-weighting and templates are the same thing, because only one free parameter is left upon imposing essential constraints. This is not the case for more complicated elements.

§31.2.4. Mass Matrix Properties

Mass matrices must satisfy certain conditions that can be used for verification and debugging. They are: (1) matrix symmetry, (2) physical symmetries, (3) conservation and (4) positivity.

Matrix Symmetry. This means $(\mathbf{M}^e)^T = \mathbf{M}^e$, which is easy to check. For a variationally derived mass matrix this follows directly from the definition (31.4), while for a DLMM is automatic.

Physical Symmetries. Element symmetries must be reflected in the mass matrix. For example, the CMM or DLMM of a prismatic bar element must be symmetric about the antidiagonal: $M_{11} = M_{22}$. To see this, flip the end nodes: the element remains the same and so does the mass matrix.

Conservation. At a minimum, total element mass must be preserved.³ This is easily verified by applying a uniform translational velocity and checking that linear momentum is conserved. Higher order conditions, such as conservation of angular momentum, are optional and not always desirable.

Positivity. For any nonzero velocity field defined by the node values $\dot{\mathbf{u}}^e \neq \mathbf{0}$, $(\dot{\mathbf{u}}^e)^T \mathbf{M}^e \dot{\mathbf{u}}^e \geq 0$. That is, \mathbf{M}^e must be nonnegative. Unlike the previous three conditions, this constraint is nonlinear in the mass matrix entries. It can be checked in two ways: through the eigenvalues of \mathbf{M}^e , or the sequence of principal minors. The second technique is more practical if the entries of \mathbf{M}^e are symbolic.

Remark 31.1. A more demanding form of the positivity constraint is to require that \mathbf{M}^e be *positive definite*: $(\dot{\mathbf{u}}^e)^T \mathbf{M}^e \dot{\mathbf{u}}^e > 0$ for any $\dot{\mathbf{u}}^e \neq \mathbf{0}$. This is more physically reassuring because one half of that quadratic form is the kinetic energy associated with the velocity field defined by $\dot{\mathbf{u}}^e$. In a continuum T can vanish only for zero velocities. But allowing $T^e = 0$ for some nonzero $\dot{\mathbf{u}}^e$ makes life easier in some situations, particularly for elements with rotational or Lagrange multiplier freedoms.

The $\dot{\mathbf{u}}^e$ for which $T^e = 0$ form the *null space* of \mathbf{M}^e . Because of the conservation requirement, a rigid velocity field (the time derivative $\dot{\mathbf{u}}_R^e$ of a rigid body mode \mathbf{u}_R^e) cannot be in the mass matrix null space, since it would imply zero mass. This scenario is dual to that of the element stiffness matrix. For the latter, $\mathbf{K}^e \mathbf{u}_R^e = \mathbf{0}$, since a rigid body motion produces no strain energy. Thus \mathbf{u}_R^e must be in the null space of the stiffness matrix.

§31.2.5. Rank and Numerical Integration

Suppose the element has a total of n_F^e freedoms. A mass matrix \mathbf{M}^e is called *rank sufficient* or of *full rank* if its rank is $r_M^e = n_F^e$. Because of the positivity requirement, a rank-sufficient mass matrix must be positive definite. Such matrices are preferred from a numerical stability standpoint.

If \mathbf{M}^e has rank $r_M^e < n_F^e$ the mass is called rank deficient by $d_M^e = n_F^e - r_M^e$. Equivalently \mathbf{M}^e is d_M^e times singular. For a numerical matrix the rank is easily computed by taking its eigenvalues and looking at how many of them are zero. The null space can be extracted by functions such as `NullSpace` in *Mathematica* without the need of computing eigenvalues.

The computation of \mathbf{M}^e by the variational formulation (31.4) is often done using Gauss numerical quadrature. Each Gauss points adds n_D to the rank, where n_D is the row dimension of the shape function matrix \mathbf{N}^e , up to a maximum of n_F^e . For most elements n_D is the same as element spatial dimensionality; that is, $n_D = 1, 2$ and 3 for $1, 2$ and 3 dimensions, respectively. This property can be used to pick the minimum Gauss integration rule that makes \mathbf{M}^e positive definite.

§31.3. Globalization

Like their stiffness counterparts, mass matrices are often developed in a local or element frame. Should globalization be necessary before merge, a congruent transformation is applied:

$$\mathbf{M}^e = (\mathbf{T}^e)^T \bar{\mathbf{M}}^e \mathbf{T}^e \quad (31.10)$$

Here $\bar{\mathbf{M}}^e$ is the element mass referred to the local frame whereas \mathbf{T}^e is the local-to-global displacement transformation matrix. Matrix \mathbf{T}^e is in principle that used for the stiffness globalization. Some procedural differences, however, must be noted. For stiffness matrices \mathbf{T}^e is often *rectangular* if the local stiffness has lower dimensionality. For example, the bar and spar elements formulated of

³ We are talking about classical mechanics here; in relativistic mechanics mass and energy can be exchanged.

Chapter 6 have 2×2 local stiffnesses. Globalization to 2D and 3D involves application of 2×4 and 2×6 transformation matrices, respectively. This works fine because the local element has zero stiffness in some directions. If the associated freedoms are explicitly kept in the local stiffness, as in Chapters 2–3, those rows and columns are zero and have no effect on the global stiffness.

In contrast to stiffnesses, *translational masses never vanish*. One way to understand this is to think of an element moving in a translational rigid body motion u_R with acceleration \ddot{u}_R . According to Newton's second law, $f_R = M^e \ddot{u}_R$, where M^e is the translational mass. This cannot be zero.

The conclusion is: *all translational masses must be retained in the local mass matrix*. The 2-node prismatic bar moving in the $\{x, y\}$ plane furnishes a simple illustration. With the freedoms arranged as $\mathbf{u}^e = [u_{x1} \ u_{y1} \ u_{x1} \ u_{y2}]^T$, the local mass matrix constructed by consistent and diagonalized lumping are

$$\bar{\mathbf{M}}_C^e = \frac{1}{6} \rho A \ell \begin{bmatrix} 2 & 0 & 1 & 0 \\ 0 & 2 & 0 & 1 \\ 1 & 0 & 2 & 0 \\ 0 & 1 & 0 & 2 \end{bmatrix}, \quad \bar{\mathbf{M}}_L^e = \frac{1}{2} \rho A \ell \begin{bmatrix} 1 & 0 & 0 & 0 \\ 0 & 1 & 0 & 0 \\ 0 & 0 & 1 & 0 \\ 0 & 0 & 0 & 1 \end{bmatrix} = \frac{1}{2} \rho A \ell \mathbf{I}_4, \quad (31.11)$$

respectively. Globalize via (31.10) using the transformation matrix (3.2). The result is $\mathbf{M}_C^e = \bar{\mathbf{M}}_C^e$ and $\mathbf{M}_L^e = \bar{\mathbf{M}}_L^e$. We say that these mass matrices *repeat*. Verification for the DLMM is easy because \mathbf{T}^e is orthogonal: $(\mathbf{T}^e)^T \bar{\mathbf{M}}_L^e \mathbf{T}^e = \frac{1}{2} \rho A \ell (\mathbf{T}^e)^T \mathbf{I}_4 \mathbf{T}^e = \frac{1}{2} \rho A \ell (\mathbf{T}^e)^T \mathbf{T}^e = \frac{1}{2} \rho A \ell \mathbf{I}_4$. For the CMM, however, repetition is not obvious. It is best shown by temporarily rearranging the element DOF so that instead of $[u_{x1} \ u_{y1} \ u_{x1} \ u_{y2}]$ the x and y components are grouped: $[u_{x1} \ u_{x2} \ u_{y1} \ u_{y2}]$. Rearranging $\bar{\mathbf{M}}_C^e$ and \mathbf{T}^e accordingly yields

$$\bar{\mathbf{M}}_C^e = \begin{bmatrix} \tilde{\mathbf{M}} & \mathbf{0} \\ \mathbf{0} & \tilde{\mathbf{M}} \end{bmatrix}, \quad \mathbf{T}^e = \begin{bmatrix} c\mathbf{I}_2 & s\mathbf{I}_2 \\ -s\mathbf{I}_2 & c\mathbf{I}_2 \end{bmatrix}, \quad \text{with } \tilde{\mathbf{M}} = \frac{\rho A \ell}{6} \begin{bmatrix} 2 & 1 \\ 1 & 2 \end{bmatrix}, \quad c = \cos \phi, \quad s = \sin \phi. \quad (31.12)$$

in which $\phi = \angle x, \bar{x}$. Carrying out the transformation in block form gives

$$\mathbf{M}_C^e = \begin{bmatrix} c\mathbf{I}_2 & -s\mathbf{I}_2 \\ s\mathbf{I}_2 & c\mathbf{I}_2 \end{bmatrix} \begin{bmatrix} \tilde{\mathbf{M}} & \mathbf{0} \\ \mathbf{0} & \tilde{\mathbf{M}} \end{bmatrix} \begin{bmatrix} c\mathbf{I}_2 & s\mathbf{I}_2 \\ -s\mathbf{I}_2 & c\mathbf{I}_2 \end{bmatrix} = \begin{bmatrix} (c^2 + s^2)\tilde{\mathbf{M}} & (cs - cs)\tilde{\mathbf{M}} \\ (cs - cs)\tilde{\mathbf{M}} & (c^2 + s^2)\tilde{\mathbf{M}} \end{bmatrix} = \begin{bmatrix} \tilde{\mathbf{M}} & \mathbf{0} \\ \mathbf{0} & \tilde{\mathbf{M}} \end{bmatrix} = \bar{\mathbf{M}}_C^e. \quad (31.13)$$

A matrix that can be put in a block diagonal form built up of identical submatrices, such as $\bar{\mathbf{M}}_C^e$ in (31.12) is called *repeating block diagonal* or RBD. Note that the contents and order of $\tilde{\mathbf{M}}$ are irrelevant to the result (31.13). Hence the following generalization follows. If upon rearranging the element DOF: (i) $\bar{\mathbf{M}}^e$ is two-block RBD, and (ii) \mathbf{T}^e takes the block form shown above, the local and global matrices will coalesce. For (ii) to hold, it is sufficient that all nodal DOF be translational and be referred to the same coordinate system. The same conclusion holds for 3D; this is the subject of Exercise 31.5. This *repetition rule* can be summarized as follows:

A RBD local mass matrix globalizes to the same matrix if all element DOFs are translational and all of them are referred to the same global system.

(31.14)

This property should be taken advantage of to skip superfluous local-to-global transformations. Frequently such operation costs more than forming the local mass matrix.

What if the (31.14) fails on actual computation? Then something (mass matrix or transformation) is wrong and must be fixed. As example, suppose that one tries to parrot the bar stiffness derivation process by starting with the 1D bar mass (31.1). A rectangular 2×4 transformation matrix \mathbf{T}^e is built by taking rows 1 and 3 of (3.2). Then the globalization (31.10) is carried out. The resulting \mathbf{M}_L^e is found to violate (31.14) because entries depend on the orientation angle $\varphi = \angle(\bar{x}, x)$. The reason for this mistake is that $\bar{\mathbf{M}}_L^e$ must account for the inertia in the y direction, as in the second of (31.11), to start with.

Remark 31.2. The repetition rule (31.14) can be expected to fail in the following scenarios:

1. The element has non-translational freedoms. (Occasionally the rule may work, but that is unlikely.)
2. The mass blocks are different in content and/or size. This occurs if different models are used in different directions. Examples are furnished by beam-column, element with curved sides or faces, and shell elements.
3. Nodes are referred to different coordinate frames in the global system. This can happen if certain nodes are referred to special frames to facilitate the application of boundary conditions.

§31.4. Mass Matrix Examples: Bars and Beams

The diagonally lumped and consistent mass matrices for the 2-node bar element were explicitly given in (31.1) and (31.5), and an optimal combination is investigated in the next Chapter. In this section the DLMM and CMM of other simple elements are worked out. More complicated ones are relegated to Exercises. The overbar of \mathbf{M}^e is omitted for brevity unless a distinction between local and global mass matrices is required.

§31.4.1. The 3-Node Bar

The element is prismatic with length ℓ , area A , and uniform mass density ρ . Midnode 3 is at the center. The DOFs are arranged $\mathbf{u}^e = [u_1 \ u_2 \ u_3]^T$. Using the shape function in the isoparametric coordinate ξ presented in Exercise 16.2 we get the CMM

$$\mathbf{M}_C^e = \rho A \int_{-1}^1 (\mathbf{N}^e)^T \mathbf{N}^e (1/2\ell) d\xi = \frac{\rho A \ell}{30} \begin{bmatrix} 4 & -1 & 2 \\ -1 & 4 & 2 \\ 2 & 2 & 16 \end{bmatrix}. \quad (31.15)$$

To produce a DLMM, the total mass of the element is divided into 3 parts: $\alpha\rho A\ell$, $\alpha\rho A\ell$, and $(1 - 2\alpha)\rho A\ell$, which are assigned to nodes 1, 2 and 3, respectively.

For reasons discussed later the best choice is $\alpha = 1/6$, as depicted in Figure 31.2. Consequently $2/3$ of the total mass goes to the midpoint, and what is left to the corners, giving

$$\mathbf{M}_L^e = \frac{1}{6}\rho A \ell \begin{bmatrix} 1 & 0 & 0 \\ 0 & 1 & 0 \\ 0 & 0 & 4 \end{bmatrix}. \quad (31.16)$$

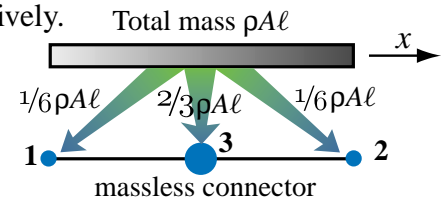


FIGURE 31.2. Direct mass lumping for 3-node bar element.

The $1/6:1/6:2/3$ allocation happens to be Simpson's rule for integration. This meshes in with the interpretation of diagonal mass lumping as a Lobatto integration rule, a topic discussed in §31.6.

Both (31.15) and (31.16) can be used as building blocks for expanding the element to 2D or 3D space. The repetition rule (31.14) holds.

```

Beam2BEConsMass[Le_,ρ_,A_,{numer_,p_}]:=
Module[{i,k,Ne,NeT,ξ,w, fac,Me=Table[0,{4},{4}]},
Ne={2*(1-ξ)^2*(2+ξ), (1-ξ)^2*(1+ξ)*Le,
2*(1+ξ)^2*(2-ξ), -(1+ξ)^2*(1-ξ)*Le}/8;
NeT=Transpose[Ne]; fac=ρ*A*Le/2;
If [p==0, Me=fac*Integrate[NeT.Ne,{ξ,-1,1}]; Return[Me]];
For [k=1, k<=p, k++,
{xi,w}= LineGaussRuleInfo[{p,numer},k];
Me+= w*fac*(NeT/.ξ->xi).(Ne/.ξ->xi);
]; If[!numer,Me=Simplify[Me]]; Return[Me]
];
ClearAll[ρ,A,Le,ξ]; mfac=(ρ*A*Le)/420;
MeC=Simplify[Beam2BEConsMass[Le,ρ,A,{False,0}]/mfac];
For [p=1,p<=5,p++, Print["p=",p];
Me=Simplify[Beam2BEConsMass[Le,ρ,A,{False,p}]/mfac];
Print["Me=",mfac,"",Me//MatrixForm,
" vs exact=",mfac,"",MeC//MatrixForm];
Print["eigs scaled ME=",Chop[Eigenvalues[N[Me/.Le->1]]]];
uRot={-Le/2,1,Le/2,1}*θ; TRot=Simplify[(1/2)*uRot.MeC.uRot*mfac];
TRotex=Simplify[(Le/2)*Integrate[(1/2)*ρ*A*(θ*Le*ξ/2)^2,{ξ,-1,1}]];
Print["TRot=",TRot," should match ",TRotex];

```

FIGURE 31.3. Module to form the CMM of a prismatic 2-node Bernoulli-Euler plane beam element. Integration is done analytically if $p=0$, and numerically if $p > 0$ using a p -point Gauss rule.

§31.4.2. The Bernoulli-Euler Plane Beam

The stiffness of this element was derived in Chapter 13. The 2-node plane beam element has length ℓ , cross section area A and uniform mass density ρ . Only the translational inertia due to the lateral motion of the beam is considered in computing the kinetic energy $T = \frac{1}{2} \int_0^\ell \rho \dot{v}(\bar{x})^2 d\bar{x}$ of the element, whereas the rotational inertia is ignored. With the freedoms arranged as $\mathbf{u}^e = [v_1 \ \theta_1 \ v_2 \ \theta_2]^T$, use of the cubic shape functions (13.12) gives the CMM

$$\bar{\mathbf{M}}_C^e = \rho A \int_{-1}^1 (1/2\ell)(\mathbf{N}^e)^T \mathbf{N}^e d\xi = \frac{\rho A \ell}{420} \begin{bmatrix} 156 & 22\ell & 54 & -13\ell \\ 22\ell & 4\ell^2 & 13\ell & -3\ell^2 \\ 54 & 13\ell & 156 & -22\ell \\ -13\ell & -3\ell^2 & -22\ell & 4\ell^2 \end{bmatrix}. \quad (31.17)$$

in which $1/2\ell$ is the Jacobian $J = dx/d\xi$. This result may be verified using the *Mathematica* module `Beam2BEConsMatrix` listed in Figure 31.3. The arguments are self-explanatory except for p . The module computes the integral (31.17) analytically if $p=0$; else using a p -point 1D Gauss rule (extracted from `LineGaussRuleInfo`, described in Chapter 17) if $1 \leq p \leq 5$. `Beam2BEConsMatrix` is run for p varying from 0 through 5 by the statements following the module. The mass matrices obtained with integration rules of 1, 2 and 3 points are

$$c_1 \begin{bmatrix} 16 & 4\ell & 16 & -4\ell \\ 4\ell & \ell^2 & 4\ell & -\ell^2 \\ 16 & 4\ell & 16 & -4\ell \\ -4\ell & -\ell^2 & -4\ell & \ell^2 \end{bmatrix}, \quad c_2 \begin{bmatrix} 86 & 13\ell & 22 & -5\ell \\ 13\ell & 2\ell^2 & 5\ell & -\ell^2 \\ 22 & 5\ell & 86 & -13\ell \\ -5\ell & -\ell^2 & -13\ell & 2\ell^2 \end{bmatrix}, \quad c_3 \begin{bmatrix} 444 & 62\ell & 156 & -38\ell \\ 62\ell & 11\ell^2 & 38\ell & -9\ell^2 \\ 156 & 38\ell & 444 & -62\ell \\ -38\ell & -9\ell^2 & -62\ell & 11\ell^2 \end{bmatrix} \quad (31.18)$$

in which $c_1 = \rho A \ell / 64$, $c_2 = \rho A \ell / 216$ and $c_3 = \rho A \ell / 1200$. The eigenvalue analysis shows that all three are singular, with rank 1, 2 and 3, respectively. The result for 4 and 5 points agrees with

(31.17), which has full rank. The purpose of this example is to illustrate the rank property quoted in §31.2.5: each Gauss point adds one to the rank (up to 4) since the problem is one-dimensional.

The matrix (31.17) conserves linear and angular momentum; the latter property being checked by the last 3 statements of Figure 31.3. So do the reduced-integration mass matrices if $p > 1$.

To get a diagonally lumped mass matrix is trickier. Obviously the translational nodal masses must be the same as that of a bar: $1/2\rho A\ell$. See Figure 31.4. But there is no consensus on rotational masses. To accommodate these variations, it is convenient to leave the latter parametrized as follows

$$\bar{\mathbf{M}}_L^e = \rho A \ell \begin{bmatrix} 1/2 & 0 & 0 & 0 \\ 0 & \alpha \ell^2 & 0 & 0 \\ 0 & 0 & 1/2 & 0 \\ 0 & 0 & 0 & \alpha \ell^2 \end{bmatrix}, \quad \alpha \geq 0. \quad (31.19)$$

Here α is a nonnegative parameter, typically between 0 and 1/50. The choice of α has been argued in the FEM literature over several decades, but the whole discussion is largely futile. Matching the angular momentum of the beam element gyrating about its midpoint gives $\alpha = -1/24$. This violates the positivity condition stated in 31.2.4. It follows that the *best possible* α — as opposed to possible best — is zero. This choice gives, however, a singular mass matrix, which is undesirable in scenarios where a mass-inverse appears.

Remark 31.3. This result can be readily understood physically. As shown in §32.3.2, the $1/2\rho A\ell$ translational end node masses grossly overestimate (by a factor of 3 in fact) the angular momentum of the element. Hence adding any rotational lumped mass only makes things worse.

§31.4.3. The Plane Beam-Column

To use the foregoing results for dynamics of a plane frame structure, such as a multistory building, the 2-node bar and plane beam elements must be combined to form a plane beam-column element with six degrees of freedom in the local system. The element is then rotated into its global position. The stiffness computation process was covered in Chapter 20. Figure 31.5, which is largely a reproduction of Figure 20.6, shows this element in its local and global configurations. In this case the global and local mass matrices are not identical because of the presence of rotational DOFs; furthermore the models in the longitudinal \bar{x} and lateral \bar{y} directions are different. Consequently the distinction between local and global masses must be carefully kept.

The local consistent mass matrix $\bar{\mathbf{M}}_C^e$ is easily obtained by augmenting (31.5) and (31.17) with zeros rows and columns to fill up missing DOFs, and adding. The local-to-global transformation matrix \mathbf{T}^e is that given in Chapter 20 and reproduced here for convenience. The two matrices are

$$\bar{\mathbf{M}}_C^e = \frac{\rho A \ell}{420} \begin{bmatrix} 140 & 0 & 0 & 70 & 0 & 0 \\ 0 & 156 & 22\ell & 0 & 54 & -13\ell \\ 0 & 22\ell & 4\ell^2 & 0 & 13\ell & -3\ell^2 \\ 70 & 0 & 0 & 140 & 0 & 0 \\ 0 & 54 & 13\ell & 0 & 156 & -22\ell \\ 0 & -13\ell & -3\ell^2 & 0 & -22\ell & 4\ell^2 \end{bmatrix}, \quad \mathbf{T}^e = \begin{bmatrix} c_\varphi & s_\varphi & 0 & 0 & 0 & 0 \\ -s_\varphi & c_\varphi & 0 & 0 & 0 & 0 \\ 0 & 0 & 1 & 0 & 0 & 0 \\ 0 & 0 & 0 & c_\varphi & s_\varphi & 0 \\ 0 & 0 & 0 & -s_\varphi & c_\varphi & 0 \\ 0 & 0 & 0 & 0 & 0 & 1 \end{bmatrix} \quad (31.20)$$

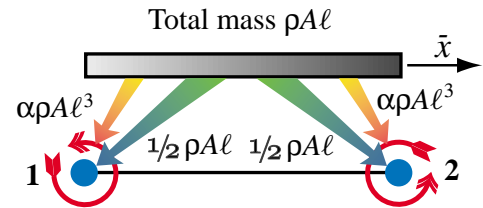


FIGURE 31.4. Direct mass lumping for 2-node Bernoulli-Euler plane beam element.

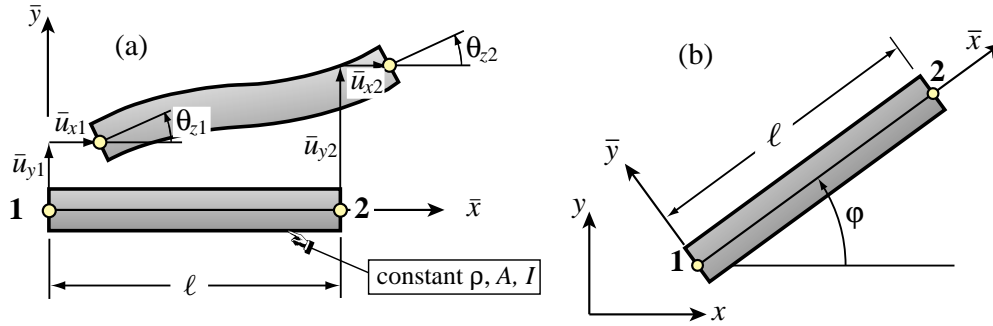


FIGURE 31.5. The 2-node plane beam-column element: (a) referred to its local system $\{\bar{x}, \bar{y}\}$; (b) referred to the global system $\{x, y\}$.

where $c_\varphi = \cos \varphi$, $s_\varphi = \sin \varphi$, and $\varphi = \angle(x, \bar{x})$, positive counterclockwise, see Figure 31.5(b). The globalized CMM is

$$\mathbf{M}_C^e = (\mathbf{T}^e)^T \bar{\mathbf{M}}_C^e \mathbf{T}^e = \frac{\rho A \ell}{420} \begin{bmatrix} 148-8c_{\varphi\varphi} & -8s_{\varphi\varphi} & -22ls_\varphi & 62+8c_{\varphi\varphi} & 8s_{\varphi\varphi} & 13ls_\varphi \\ -8s_{\varphi\varphi} & 148+8c_{\varphi\varphi} & 22lc_\varphi & 8s_{\varphi\varphi} & 62-8c_{\varphi\varphi} & -13lc_\varphi \\ -22ls_\varphi & 22lc_\varphi & 4\ell^2 & -13ls_\varphi & 13lc_\varphi & -3\ell^2 \\ 62+8c_{\varphi\varphi} & 8s_{\varphi\varphi} & -13ls & 148-8c_{\varphi\varphi} & -8s_{\varphi\varphi} & 22ls_\varphi \\ 8s_{\varphi\varphi} & 62-8c_{\varphi\varphi} & 13lc_\varphi & -8s_{\varphi\varphi} & 148+8c_{\varphi\varphi} & -22lc_\varphi \\ 13ls_\varphi & -13lc_\varphi & -3\ell^2 & 22ls_\varphi & -22lc_\varphi & 4\ell^2 \end{bmatrix} \quad (31.21)$$

in which $c_{\varphi\varphi} = \cos 2\varphi$ and $s_{\varphi\varphi} = \sin 2\varphi$. The global and local matrices differ for arbitrary φ . It may be verified, however, that $\bar{\mathbf{M}}_C^e$ and \mathbf{M}_C^e have the same eigenvalues, since \mathbf{T}^e is orthogonal.

§31.4.4. *The Timoshenko Plane Beam

The Timoshenko plane beam model for static analysis was presented as advanced material in Chapter 13.

This model is more important for dynamics and vibration than Bernoulli-Euler, and indispensable for short transient and wave propagation analysis. (As remarked in **Notes and Bibliography** of Chapter 13, the Bernoulli-Euler beam has infinite phase velocity, because the equation of motion is parabolic, and thus useless for simulating wave propagation.) The Timoshenko beam incorporates two refinements over the Bernoulli-Euler model:

1. For both statics and dynamics: plane sections remain plane but not necessarily normal to the deflected midsurface. See Figure 31.6. This assumption allows the averaged shear distortion to be included in both strain and kinetic energies.
2. In dynamics: the rotary inertia is included in the kinetic energy.

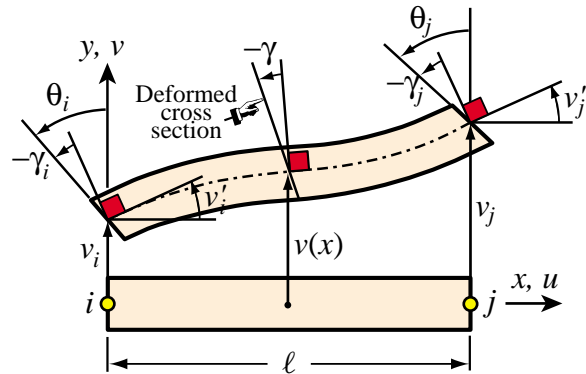


FIGURE 31.6. Kinematic assumptions of the Timoshenko plane beam element. (A reproduction of Figure 13.14 for the reader convenience.)

According to the second assumption, the kinetic energy of the Timoshenko beam element is given by

$$T = \frac{1}{2} \int_0^\ell (\rho A \dot{v}(x)^2 + \rho I_R \dot{\theta}(x)^2) dx. \quad (31.22)$$

Here I_R is the second moment of inertia to be used in the computation of the rotary inertia and $\theta = v' + \gamma$ is the cross-section rotation angle shown in Figure 31.6; $\gamma = V/(GA_s)$ being the section-averaged shear distortion. The element DOF are ordered $\mathbf{u}^e = [v_1 \ \theta_1 \ v_2 \ \theta_2]^T$. The lateral displacement interpolation is

$$v(\xi) = v_1 N_{v1}^e(\xi) + v_1' N_{v1'}^e(\xi) + v_2 N_{v2}^e(\xi) + v_2' N_{v2'}^e(\xi), \quad \xi = \frac{2x}{\ell} - 1, \quad (31.23)$$

in which the cubic interpolation functions (13.12) are used. A complication over Bernoulli-Euler is that the rotational freedoms are θ_1 and θ_2 but the interpolation (31.23) is in terms of the neutral surface end slopes: $v_1' = (dv/dx)_1 = \theta_1 - \gamma$ and $v_2' = (dv/dx)_2 = \theta_2 - \gamma$. From the analysis of §13.7 we can derive the relation

$$\begin{bmatrix} v_1' \\ v_2' \end{bmatrix} = \frac{1}{1 + \Phi} \begin{bmatrix} -\frac{\Phi}{\ell} & 1 + \frac{\Phi}{2} & \frac{\Phi}{\ell} & -\frac{\Phi}{2} \\ -\frac{\Phi}{\ell} & -\frac{\Phi}{2} & \frac{\Phi}{\ell} & 1 + \frac{\Phi}{2} \end{bmatrix} \begin{bmatrix} v_1 \\ \theta_1 \\ v_2 \\ \theta_2 \end{bmatrix}. \quad (31.24)$$

where as in (13.22) the dimensionless parameter $\Phi = 12EI/(GA_s \ell^2)$ characterizes the ratio of bending and shear rigidities. The end slopes of (31.24) are replaced into (31.23), the interpolation for θ obtained, and v and θ inserted into the kinetic energy (31.22). After lengthy algebra the CMM emerges as the sum of two contributions:

$$\mathbf{M}_C^e = \mathbf{M}_{CT}^e + \mathbf{M}_{CR}^e, \quad (31.25)$$

where \mathbf{M}_{CT} and \mathbf{M}_{CR} accounts for the translational and rotary inertia, respectively:

$$\mathbf{M}_{CT}^e = \frac{\rho A \ell}{(1 + \Phi)^2} \begin{bmatrix} \frac{13}{35} + \frac{7}{10} \Phi + \frac{1}{3} \Phi^2 & (\frac{11}{210} + \frac{11}{120} \Phi + \frac{1}{24} \Phi^2) \ell & \frac{9}{70} + \frac{3}{10} \Phi + \frac{1}{6} \Phi^2 & -(\frac{13}{420} + \frac{3}{40} \Phi + \frac{1}{24} \Phi^2) \ell \\ & (\frac{1}{105} + \frac{1}{60} \Phi + \frac{1}{120} \Phi^2) \ell^2 & (\frac{13}{420} + \frac{3}{40} \Phi + \frac{1}{24} \Phi^2) \ell & -(\frac{1}{140} + \frac{1}{60} \Phi + \frac{1}{120} \Phi^2) \ell^2 \\ \text{symmetric} & & \frac{13}{35} + \frac{7}{10} \Phi + \frac{1}{3} \Phi^2 & (\frac{11}{210} + \frac{11}{120} \Phi + \frac{1}{24} \Phi^2) \ell \\ & & & (\frac{1}{105} + \frac{1}{60} \Phi + \frac{1}{120} \Phi^2) \ell^2 \end{bmatrix}$$

$$\mathbf{M}_{CR}^e = \frac{\rho I_R}{(1 + \Phi)^2 \ell} \begin{bmatrix} \frac{6}{5} & (\frac{1}{10} - \frac{1}{2} \Phi) \ell & -\frac{6}{5} & (\frac{1}{10} - \frac{1}{2} \Phi) \ell \\ & (\frac{2}{15} + \frac{1}{6} \Phi + \frac{1}{3} \Phi^2) \ell^2 & (-\frac{1}{10} + \frac{1}{2} \Phi) \ell & -(\frac{1}{30} + \frac{1}{6} \Phi - \frac{1}{6} \Phi^2) \ell^2 \\ \text{symmetric} & & \frac{6}{5} & (-\frac{1}{10} + \frac{1}{2} \Phi) \ell \\ & & & (\frac{2}{15} + \frac{1}{6} \Phi + \frac{1}{3} \Phi^2) \ell^2 \end{bmatrix} \quad (31.26)$$

Caveat: the I in $\Phi = 12EI/(GA_s \ell^2)$ is the second moment of inertia that enters in the elastic flexural elastic rigidity defined in (13.5). If the beam is homogeneous $I_R = I$, but that is not necessarily the case if, as sometimes happens, the beam has nonstructural attachments that contribute rotary inertia.

The factor of \mathbf{M}_{CR}^e can be further transformed to facilitate parametric studies by introducing $r_R^2 = I_R/A$ as cross-section gyration radius and $\Psi = r_R/\ell$ as element slenderness ratio. Then the factor $\rho I_R/((1 + \Phi)^2 \ell)$ becomes $\rho A \ell \Psi^2/(1 + \Phi)^2$. If $\Phi = 0$ and $\Psi = 0$, \mathbf{M}_{CR}^e vanishes and \mathbf{M}_{CT}^e in (31.26) reduces to (31.17).

Obtaining a diagonally lumped matrix can be done by the HRZ scheme explained in 31.6.1. The optimal lumped mass is derived in the next Chapter by the template method.

§31.4.5. *Spar and Shaft Elements

The mass matrices for these 2-node elements are very similar to those of the bar, since they can be derived from linear displacement interpolation for the CMM. The only thing that changes is the matrix factor and the end DOFs. The derivation of these elements is done as Exercises.

```

Trig3IsoPMembraneConsMass[ncoor_, ρ_, h_, {numer_, p_}] :=
Module[{i, k, x1, y1, x2, y2, x3, y3, A, Nfxy,
      tcoor, w, Me = Table[0, {6}, {6}]},
  For [k=1, k<=Abs[p], k++,
    {{x1, y1}, {x2, y2}, {x3, y3}} = ncoor;
    A = Simplify[(x2-x1)*(y3-y1) - (x1-x3)*(y1-y2)]/2;
    {tcoor, w} = TrigGaussRuleInfo[{p, numer}, k];
    Nfxy = {Flatten[Table[{tcoor[[i]], 0}, {i, 3}]],
            Flatten[Table[{0, tcoor[[i]]}, {i, 3}]]};
    Me += ρ*w*A*h*Transpose[Nfxy].Nfxy;
  ]; If[!numer, Me = Simplify[Me]]; Return[Me]
];

```

FIGURE 31.7. CMM module for 3-node linear triangle in plane stress.

§31.5. Mass Matrix Examples: Plane Stress

To illustrate the two-dimensional case, this section works out the mass matrices of two simple plane stress elements. More complicated cases are relegated to the Exercises.

§31.5.1. The Plane Stress Linear Triangle

The stiffness formulation of the 3-node triangle was discussed in Chapter 15. For the following derivations the plate is assumed to have constant mass density ρ , area A , uniform thickness h , and motion restricted to the $\{x, y\}$ plane. The six DOFs are arranged as $\mathbf{u}^e = [u_{x1} \ u_{y1} \ u_{x2} \ u_{y2} \ u_{x3} \ u_{y3}]^T$. The consistent mass matrix is obtained using the linear displacement interpolation (15.17). Expanding $(\mathbf{N}^e)^T \mathbf{N}^e$ gives a 6×6 matrix quadratic in the triangular coordinates. This can be integrated with the formulas (15.27) exemplified by $\int_{\Omega^e} \zeta_1^2 d\Omega = A/3$, $\int_{\Omega^e} \zeta_1 \zeta_2 d\Omega = A/6$, etc. The result is

$$\mathbf{M}_C^e = \rho h \int_{\Omega^e} \begin{bmatrix} \zeta_1 \zeta_1 & 0 & \zeta_1 \zeta_2 & 0 & \zeta_1 \zeta_3 & 0 \\ 0 & \zeta_1 \zeta_1 & 0 & \zeta_1 \zeta_2 & 0 & \zeta_1 \zeta_3 \\ \zeta_2 \zeta_1 & 0 & \zeta_2 \zeta_2 & 0 & \zeta_2 \zeta_3 & 0 \\ 0 & \zeta_2 \zeta_1 & 0 & \zeta_2 \zeta_2 & 0 & \zeta_2 \zeta_3 \\ \zeta_3 \zeta_1 & 0 & \zeta_3 \zeta_2 & 0 & \zeta_3 \zeta_3 & 0 \\ 0 & \zeta_3 \zeta_1 & 0 & \zeta_3 \zeta_2 & 0 & \zeta_3 \zeta_3 \end{bmatrix} d\Omega = \frac{\rho Ah}{12} \begin{bmatrix} 2 & 0 & 1 & 0 & 1 & 0 \\ 0 & 2 & 0 & 1 & 0 & 1 \\ 1 & 0 & 2 & 0 & 1 & 0 \\ 0 & 1 & 0 & 2 & 0 & 1 \\ 1 & 0 & 1 & 0 & 2 & 0 \\ 0 & 1 & 0 & 1 & 0 & 2 \end{bmatrix} \quad (31.27)$$

This computation may be checked with the *Mathematica* module listed in Figure 31.7. The module is invoked as `Trig3IsoPMembraneConsMass[ncoor, ρ, h, {numer, p}]` and returns matrix `Me`. The arguments are: `ncoor` passes the node coordinate list $\{\{x_1, y_1\}, \{x_2, y_2\}, \{x_3, y_3\}\}$, ρ the mass density, h the plate thickness, `numer` is a logical flag set to `True` or `False` for numeric or symbolic computations, respectively, and `p` identifies the triangle integration rule as described in §24.2.1. Subordinate module `TrigGaussRuleInfo` is described in Chapter 24. Since the order of \mathbf{M}^e is 6, and each Gauss point adds two (the number of space dimensions) to the rank, a rule with 3 or more points is required to reach full rank, as can be verified by simple numerical experiments.

The lumped mass matrix is constructed by taking the total mass of the element, which is ρAh , dividing it by 3 and assigning those to the corner nodes. See Figure 31.8. This process produces a

diagonal matrix:

$$\mathbf{M}_L^e = \frac{\rho Ah}{3} \mathbf{diag}[1 \ 1 \ 1 \ 1 \ 1 \ 1] = \frac{\rho Ah}{3} \mathbf{I}_6. \quad (31.28)$$

The same matrix is obtained by any other diagonalization method.

Remark 31.4. If this element is used in three dimensions (for example as membrane component of a shell element), it is necessary to insert the normal-to-the-plate z mass components in either (31.27) or (31.28). According to the invariance rule (31.14) the globalization process is trivial because \mathbf{M}_C^e or \mathbf{M}_L^e becomes RBD on grouping the element DOFs by component. Thus the local element mass matrix repeats in the global frame.

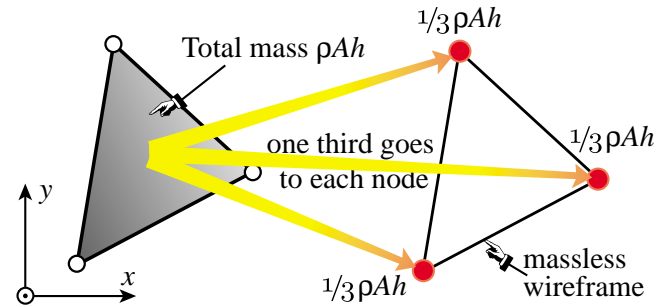


FIGURE 31.8. DLMM for 3-node triangular element.

```

Quad4IsoPMembraneCMass[ncoor_,rho_,h_,{numer_,p_}]:=
Module[{i,k,Nf,dNx,dNy,Jdet,Nfxy,qcoor,w,Me=Table[0,{8},{8}]},
For[k=1,k<=p*p,k++,
{qcoor,w}=QuadGaussRuleInfo[{p,numer},k];
{Nf,dNx,dNy,Jdet}=Quad4IsoPShapeFunDer[ncoor,qcoor];
Nfxy={Flatten[Table[{Nf[[i]],0},{i,4]}],
Flatten[Table[{0,Nf[[i]]},{i,4]}]};
Me+=(rho*w*Jdet*h/2)*Transpose[Nfxy].Nfxy;
];If[!numer,Me=Simplify[Me]];Return[Me]
];

```

FIGURE 31.9. CMM module for 4-node bilinear quad in plane stress.

§31.5.2. Four-Node Bilinear Quadrilateral

Module `Quad4IsoPMembraneConsMass`, listed in Figure 31.9, returns the CMM of a 4-node bilinear quadrilateral under plane stress, moving in the $\{x, y\}$ plane. The plate is homogeneous with density ρ and constant thickness h . The arguments are similar to those described for the linear triangle, except that the quadrature rule pertains to quadrilaterals, and is specified as described in Chapter 23. The subordinate modules `QuadGaussRuleInfo` (shape functions) and `Quad4IsoPShapeFunDer` (Gauss quadrature information) are described in that Chapter.

The integration is carried out numerically using a $p \times p$ Gauss product rule, with p specified as argument. Testing the module on a rectangular element of dimensions $\{a, b\}$ returns the following CMMs for the 1×1 and 2×2 Gauss rules:

$$\mathbf{M}_{C1 \times 1}^e = \frac{\rho abh}{32} \begin{bmatrix} 1 & 0 & 1 & 0 & 1 & 0 & 1 & 0 \\ 0 & 1 & 0 & 1 & 0 & 1 & 0 & 1 \\ 1 & 0 & 1 & 0 & 1 & 0 & 1 & 0 \\ 0 & 1 & 0 & 1 & 0 & 1 & 0 & 1 \\ 1 & 0 & 1 & 0 & 1 & 0 & 1 & 0 \\ 0 & 1 & 0 & 1 & 0 & 1 & 0 & 1 \\ 1 & 0 & 1 & 0 & 1 & 0 & 1 & 0 \\ 0 & 1 & 0 & 1 & 0 & 1 & 0 & 1 \end{bmatrix}, \quad \mathbf{M}_{C2 \times 2}^e = \frac{\rho abh}{72} \begin{bmatrix} 4 & 0 & 2 & 0 & 1 & 0 & 2 & 0 \\ 0 & 4 & 0 & 2 & 0 & 1 & 0 & 2 \\ 2 & 0 & 4 & 0 & 2 & 0 & 1 & 0 \\ 0 & 2 & 0 & 4 & 0 & 2 & 0 & 1 \\ 1 & 0 & 2 & 0 & 4 & 0 & 2 & 0 \\ 0 & 1 & 0 & 2 & 0 & 4 & 0 & 2 \\ 2 & 0 & 1 & 0 & 2 & 0 & 4 & 0 \\ 0 & 2 & 0 & 1 & 0 & 2 & 0 & 4 \end{bmatrix}. \quad (31.29)$$

The mass given by 1-point integration has rank 2 and 6 zero eigenvalues, and thus rank-deficient by 6. The mass given by the 2×2 rule is rank-sufficient and positive definite. Either matrix repeats on globalization. Using $p > 2$ returns $\mathbf{M}_{C2 \times 2}^e$. The DLMM is obtained by assigning one fourth of the total element mass ρabh to each freedom.

§31.6. Mass Diagonalization Methods

The construction of consistent mass matrix (CMM) is fully defined by the choice of kinetic energy functional and shape functions. No procedural deviation is possible. On the other hand the construction of a diagonally lumped mass matrix (DLMM) is not a unique process, except for very simple elements in which the lumping is fully defined by conservation and symmetry considerations. A consequence of this ambiguity is that various methods have been proposed in the literature, ranging from heuristic through more scientific. This subsection gives a quick overview of the two more important methods.

§31.6.1. HRZ Lumping

This scheme is acronymed after the authors of [131]. It produces a DLMM given the CMM. Let M^e denote the total element mass. The procedure is as follows.

1. For each coordinate direction, select the DOFs that contribute to motion in that direction. From this set, separate translational DOF and rotational DOF subsets.
2. Add up the CMM diagonal entries pertaining to the translational DOF subset only. Call the sum S .
3. Apportion M^e to DLMM entries of both subsets on dividing the CMM diagonal entries by S .
4. Repeat for all coordinate directions.

Example 31.1. The see HRZ in action, consider the 3-node prismatic bar with CMM given by (31.15). Only one direction (x) is involved and all DOFs are translational. Excluding the factor $\rho A \ell / 30$, which does not affect the results, the diagonal entries are 4, 4 and 16, which add up to $S = 24$. Apportion the total element mass $\rho A \ell$ to nodes with weights $4/S = 1/6$, $4/S = 1/6$ and $16/S = 2/3$. The result is the DLMM (31.16).

Example 31.2. Next consider the 2-node Bernoulli-Euler plane beam element. Again only one direction (y) is involved but now there are translational and rotational freedoms. Excluding the factor $\rho A \ell / 420$, the diagonal entries of the CMM (31.17), are 156, $4\ell^2$, 156 and $4\ell^2$. Add the translational DOF entries: $S = 156 + 156 = 312$. Apportion the element mass $\rho A \ell$ to the four DOFs with weights $156/312 = 1/2$, $4\ell^2/312 = \ell^2/78$, $156/312 = 1/2$ and $4\ell^2/312 = \ell^2/78$. The result is the DLMM (31.19) with $\alpha = 1/78$.

The procedure is heuristic but widely used on account of three advantages: easy to explain and implement, applicable to any element as long as a CMM is available, and retaining nonnegativity. The last attribute is particularly important: it means that the DLMM is physically admissible, precluding numerical instability headaches. As a general assessment, it gives reasonable results if the element has only translational freedoms. If there are rotational freedoms the results can be poor compared to templates.

§31.6.2. Lobatto Lumping

A DLMM with n_F^e diagonal entries m_i is formally equivalent to a numerical integration formula with n_F^e points for the element kinetic energy:

$$T^e = \sum_{i=1}^{n_F^e} m_i T_i, \quad \text{where} \quad T_i = \frac{1}{2} \dot{u}_i^2 \quad (31.30)$$

Table 31.1. One-Dimensional Lobatto Integration Rules

<i>Points</i>	<i>Abscissas</i> $\xi_i \in [-1, 1]$	<i>Weights</i> w_i	<i>Comments</i>
2	$-\xi_1 = 1 = \xi_2$	$w_1 = w_2 = 1$	Trapezoidal rule
3	$-\xi_1 = 1 = \xi_3, \xi_2 = 0$	$w_1 = w_3 = \frac{1}{3}, w_2 = \frac{4}{3}$	Simpson's rule
4	$-\xi_1 = 1 = \xi_4, -\xi_2 = 1/\sqrt{5} = \xi_3$	$w_1 = w_4 = \frac{1}{6}, w_2 = w_3 = \frac{5}{6}$	Interior points at ± 0.447214
The 4-point Lobatto rule should not be confused with "Simpson's Three-Eighths rule," a Newton-Coates quadrature that has equidistant abscissas: $-\xi_1 = \xi_2 = 1, -\xi_3 = \xi_4 = \frac{1}{3}, w_1 = w_2 = \frac{1}{4}, w_3 = w_4 = \frac{3}{4}$.			
For $4 < n \leq 10$, which is rarely important in FEM work, see Table 25.6 of [1].			

If the element is one-dimensional and has only translational DOF, (31.30) can be placed in correspondence with the so-called *Lobatto quadrature* in numerical analysis.⁴ A Lobatto rule is a 1D Gaussian quadrature formula in which the endpoints of the interval $\xi \in [-1, 1]$ are sample points. If the formula has $p \geq 2$ abscissas, only $p - 2$ of those are free. Abscissas are symmetric about the origin $\xi = 0$ and all weights are positive. The general form is

$$\int_{-1}^1 f(\xi) d\xi = w_1 f(-1) + w_p f(1) + \sum_{i=2}^{p-1} w_i f(\xi_i). \quad (31.31)$$

The rules for $p = 2, 3, 4$ are collected in Table 31.1. Comparing (31.30) with (31.31) clearly indicates that if the nodes of a 1D element are placed at the Lobatto abscissas, the diagonal masses m_i are simply the weights w_i . This fact was first noted by Fried and Malkus [103] and further explored in [164,165]. For the type of elements noted, the equivalence works well for $p = 2, 3$. For $p = 4$ a minor difficulty arises: the interior Lobatto points are not at the thirdpoints, as can be seen in Table 31.1. If instead the element has nodes at the thirdpoints $\xi = \pm \frac{1}{3}$, one must switch to the "Simpson three-eighths" rule also listed in that Table, and adjust the masses accordingly.

As a generalization to multiple dimensions, for conciseness we call "FEM Lobatto quadrature" one in which the *connected nodes* of an element are sample points of an integration rule. The equivalence with (31.30) still holds. But the method runs into some difficulties:

Zero or Negative Masses. If one insists in higher order accuracy, the weights of 2D and 3D Lobatto rules are not necessarily positive. See for example the case of the 6-node triangle in the Exercises. This shortcoming can be alleviated, however, by accepting lower accuracy, or by sticking to product rules in geometries that permit them. See Exercise 31.19.

Rotational Freedoms. If the element has rotational DOF, Lobatto rules do not exist. Any attempt to transform rules such as (31.31) to node rotations inevitably leads to coupling.

Varying Properties. If the element is nonhomogeneous or has varying properties (for instance, a tapered bar element) the construction of Lobatto rules runs into difficulties, since the problem effectively becomes the construction of a quadrature formula with non-unity kernel.

As a general assessment, the Lobatto integration technique seems advantageous only when the mass diagonalization problem happens to fit a rule already available in handbooks such as [227].

⁴ Also called Radau quadrature by some authors, e.g. [37]. However the handbook [1, p. 888] says that Lobatto and Radau rules are slightly different.

Notes and Bibliography

The first appearance of a mass matrix in a journal article occurs in two early-1930s papers⁵ by Duncan and Collar [59,60]. There it is called “inertia matrix” and denoted by $[m]$. The original example [59, p. 869] displays the 3×3 diagonal mass of a triple pendulum. In the book [102] the notation changes to A .

Diagonally lumped mass matrices (DLMM) dominate pre-1963 work. Computational simplicity was not the only reason. Direct lumping gives an obvious way to account for *nonstructural masses* in simple discrete models of the spring-dashpot-pointmass variety. For example, in a multistory building “stick model” wherein each floor is treated as one DOF in lateral sway under earthquake or wind action, it is natural to take the entire mass of the floor (including furniture, isolation, etc.) and assign it to that freedom. Nondiagonal masses pop-up occasionally in aircraft matrix analysis — e.g. wing oscillations in [102, §10.11] — as a result of measurements. As such they necessarily account for nonstructural masses due to fuel, control equipment, etc.

The formulation of the consistent mass matrix (CMM) by Archer [11,12] was a major advance. All CMMs displayed in §31.3 were first derived in those papers. The underlying idea is old. In fact it follows directly from the 18th-Century Lagrange dynamic equations [150], a proven technique to produce generalized masses. If T is the kinetic energy of a discrete system and $\dot{u}_i(x_i)$ the velocity field defined by the nodal velocities collected in $\dot{\mathbf{u}}$, the master (system-level) \mathbf{M} can be generally defined as the Hessian of T with respect to nodal velocities:

$$T = \frac{1}{2} \int_{\Omega} \rho \dot{u}_i \dot{u}_i d\Omega, \quad u_i = u_i(\dot{\mathbf{u}}), \quad \mathbf{M} = \frac{\partial^2 T}{\partial \dot{\mathbf{u}} \partial \dot{\mathbf{u}}}. \quad (31.32)$$

This matrix is constant if T is quadratic in $\dot{\mathbf{u}}$. Two key decisions remain before this could be used in FEM.

Localization: (31.32) is applied element by element, and the master \mathbf{M} assembled by the standard DSM steps.

Interpolation: the velocity field is defined by the same element shape functions as the displacement field.

These had to wait until three things became well established by the early 1960s: (i) the Direct Stiffness Method, (ii) the concept of shape functions, and (iii) the FEM connection to Rayleigh-Ritz. The critical ingredient (iii) was established in Melosh’s thesis [174] under Harold Martin. The link to dynamics was closed with Archer’s contributions, and CMM became a staple of FEM. But only a loose staple. Problems persisted:

- (a) Nonstructural masses are not naturally handled by CMM. In systems such as ships or aircraft, the structural mass is only a fraction (10 to 20%) of the total.
- (b) It is inefficient in some solution processes, notably explicit dynamics.⁶
- (c) It may not give the best results compared to other alternatives.⁷
- (d) For elements derived outside the assumed-displacement framework, the stiffness shape functions may be unknown or be altogether missing.

Problem (a) can be addressed by constructing “rigid mass elements” accounting for inertia (and possibly gravity or centrifugal forces) but no stiffness. Nodes of these elements must be linked to structural (elastic)

⁵ The brain behind these developments, which launched Matrix Structural Analysis as narrated in Appendix H, was Arthur Collar. But in the hierarchically rigid British system of the time his name, on account of less seniority, had to be last.

⁶ In explicit time integration, accelerations are computed at the global level as $\mathbf{M}^{-1}\mathbf{f}_d$, where \mathbf{f}_d is the effective dynamic force. This is efficient if \mathbf{M} is diagonal (and nonsingular). If \mathbf{M} is the CMM, a system of equations has to be solved; moreover the stable timestep generally decreases.

⁷ If \mathbf{K} results from a conforming displacement interpolation, pairing it with the CMM is a form of Rayleigh-Ritz, and thus guaranteed to provide upper bounds on natural frequencies. This is not necessarily a good thing. In practice it is observed that errors increase rapidly as one moves up the frequency spectrum. If the response is strongly influenced by intermediate and high frequencies, as in wave propagation dynamics, the CMM may give extremely bad results.

nodes by MFC constraints that enforce kinematic constraints. This is more of an implementation issue than a research topic, although numerical difficulties typical of rigid body dynamics may crop up.

Problems (b,c,d) can be attacked by parametrization. The father of NASTRAN, Dick MacNeal, was the first to observe [157,163] that averaging the DLMM and CMM of the 2-node bar element produced better results than using either alone. This idea was further studied by Belytschko and Mullen [20] using Fourier analysis. Krieg and Key [149] had emphasized that in transient analysis the introduction of a time discretization operator brings new compensation phenomena, and consequently the time integrator and the mass matrix should not be chosen separately.

A good discussion of mass diagonalization schemes can be found in the textbook by Cook et al. [48].

The template approach addresses the problems by allowing and encouraging full customization of the mass to the problem at hand. It was first described in [82,85] for a Bernoulli-Euler plane beam using Fourier methods. It is presented in more generality in the following Chapter, where it is applied to other elements. The general concept of template as parametrized form of FEM matrices is discussed in [81].

References

Referenced items have been moved to Appendix R.

Homework Exercises for Chapter 31
Lumped and Consistent Mass Matrices

EXERCISE 31.1 [A/C:15]. Derive the consistent mass for a 2-node tapered bar element of length ℓ and constant mass density ρ , moving along its axis x , if the cross section area varies as $A = \frac{1}{2}A_1(1-\xi) + \frac{1}{2}A_2(1+\xi)$. Obtain also the DLMM by the HRZ scheme. Show that

$$\mathbf{M}_C^e = \frac{\rho\ell}{12} \begin{bmatrix} 3A_1 + A_2 & A_1 + A_2 \\ A_1 + A_2 & A_1 + 3A_2 \end{bmatrix}, \quad \mathbf{M}_L^e = \frac{\rho\ell}{8(A_1 + A_2)} \begin{bmatrix} 3A_1 + A_2 & 0 \\ 0 & A_1 + 3A_2 \end{bmatrix}. \quad (\text{E31.1})$$

EXERCISE 31.2 [A:15]. Dr. I. M. Clueless proposed a new diagonally lumped mass scheme for the 2-node bar: placing one half of the element mass $\rho A\ell$ at each Gauss point $\xi = \pm 1/\sqrt{3}$ of a two-point rule. His argument is that this configuration conserves total mass and angular momentum, which is true. Explain in two sentences why the idea is worthless.

EXERCISE 31.3 [A:25]. Extend the result (31.13) to three dimensions. The element has n^e nodes and three translational DOF per node. Arrange the element DOFs by component: \mathbf{M}^e is RBD, formed by three $n^e \times n^e$ submatrices $\tilde{\mathbf{M}}$, which are left arbitrary. For \mathbf{T}^e , assume nine blocks $t_{ij}\mathbf{I}$ for $\{i, j\} = 1, 2, 3$, where t_{ij} are the direction cosines of the local system $\{\bar{x}, \bar{y}, \bar{z}\}$ with respect to the global system $\{x, y, z\}$, and \mathbf{I} is the $n^e \times n^e$ identity matrix. Hint: use the orthogonality properties of the t_{ij} : $t_{ij}t_{ik} = \delta_{jk}$.

EXERCISE 31.4 [A:20]. Show that the local and global mass matrices of elements with only translational DOFs repeat under these constraints: all local DOFs are referred to the same local frame, and all global DOF are referred to the same global frame. Hints: the kinetic energy must be the same in both frames, and the local-to-global transformation matrix is orthogonal.

EXERCISE 31.5 [A/C:25]. Derive the CMM and DLMM for the 2-node spar and shaft elements derived in Chapter 6. Assume that the elements are prismatic with constant properties along their length ℓ .

EXERCISE 31.6 [A/C:20]. Derive the consistent mass for a 2-node Bernoulli-Euler tapered plane beam element of length ℓ if the cross section area varies as $A = A_i(1-\xi)/2 + A_j(1+\xi)/2$ while the mass density ρ is constant. Show that

$$\mathbf{M}_C^e = \frac{\rho\ell}{840} \begin{bmatrix} 240A_i + 72A_j & 2(15A_i + 7A_j)\ell & 54(A_i + A_j) & -2(7A_i + 6A_j)\ell \\ 2(15A_i + 7A_j)\ell & (5A_i + 3A_j)\ell^2 & 2(6A_i + 7A_j)\ell & -3(A_i + A_j)\ell^2 \\ 54(A_i + A_j) & 2(6A_i + 7A_j)\ell & 72A_i + 240A_j & -2(7A_i + 15A_j)\ell \\ -2(7A_i + 6A_j)\ell & -3(A_i + A_j)\ell^2 & -2(7A_i + 15A_j)\ell & (3A_i + 5A_j)\ell^2 \end{bmatrix}. \quad (\text{E31.2})$$

EXERCISE 31.7 [A:15]. Derive the local CMM and DLMM for the 2-node spar element derived in Chapter 6. Assume that the element is prismatic with constant properties along their length ℓ , and that can move in 3D space.

EXERCISE 31.8 [A:15]. Derive the local CMM and DLMM for the 2-node spar shaft derived in Chapter 6. Assume that the element is prismatic with constant properties along their length ℓ , and that can move in 3D space.

EXERCISE 31.9 [C:25]. Write a *Mathematica* script to verify the result (31.25)–(31.26). (Dont try this by hand.)

EXERCISE 31.10 [A/C:20]. Derive the consistent mass for a plane stress 3-node linear triangle with constant mass density ρ and linearly varying thickness h defined by the corner values h_1, h_2 and h_3 .

EXERCISE 31.11 [A/C:20]. Derive the consistent mass for a plane stress 6-node quadratic triangle with constant mass density ρ and uniform thickness h , moving in the $\{x, y\}$ plane. The triangle has straight sides and side nodes placed at the midpoints; consequently the metric (and thus the Jacobian) is constant. Show that with the element DOFs arranged $\mathbf{u}^e = [u_{x1} \ u_{y1} \ u_{x2} \ \dots \ u_{y6}]^T$, the CMM is [65, p. 35]

$$\mathbf{M}_C^e = \frac{\rho h A}{180} \begin{bmatrix} 6 & 0 & -1 & 0 & -1 & 0 & 0 & 0 & -4 & 0 & 0 & 0 \\ 0 & 6 & 0 & -1 & 0 & -1 & 0 & 0 & 0 & -4 & 0 & 0 \\ -1 & 0 & 6 & 0 & -1 & 0 & 0 & 0 & 0 & 0 & -4 & 0 \\ 0 & -1 & 0 & 6 & 0 & -1 & 0 & 0 & 0 & 0 & 0 & -4 \\ -1 & 0 & -1 & 0 & 6 & 0 & -4 & 0 & 0 & 0 & 0 & 0 \\ 0 & -1 & 0 & -1 & 0 & 6 & 0 & -4 & 0 & 0 & 0 & 0 \\ 0 & 0 & 0 & 0 & -4 & 0 & 32 & 0 & 16 & 0 & 16 & 0 \\ 0 & 0 & 0 & 0 & 0 & -4 & 0 & 32 & 0 & 16 & 0 & 16 \\ -4 & 0 & 0 & 0 & 0 & 0 & 16 & 0 & 32 & 0 & 16 & 0 \\ 0 & -4 & 0 & 0 & 0 & 0 & 0 & 16 & 0 & 32 & 0 & 16 \\ 0 & 0 & -4 & 0 & 0 & 0 & 16 & 0 & 16 & 0 & 32 & 0 \\ 0 & 0 & 0 & -4 & 0 & 0 & 0 & 16 & 0 & 16 & 0 & 32 \end{bmatrix} \quad (\text{E31.3})$$

and check that all eigenvalues are positive. Hint: use the shape functions of Chapter 24 and the 6 or 7-point triangle integration rule.

EXERCISE 31.12 [A:20=5+15]. Assuming the result (E31.3), use the HRZ and Lobatto integration methods to get two DLMMs for the six-node plane stress triangle. Show that HRZ gives

$$\mathbf{M}_L^e = \frac{\rho h A}{57} \mathbf{diag}[3 \ 3 \ 3 \ 3 \ 3 \ 3 \ 16 \ 16 \ 16 \ 16 \ 16 \ 16], \quad (\text{E31.4})$$

whereas Lobatto integration, using the triangle midpoint rule (24.6), gives

$$\mathbf{M}_L^e = \frac{\rho h A}{3} \mathbf{diag}[0 \ 0 \ 0 \ 0 \ 0 \ 0 \ 1 \ 1 \ 1 \ 1 \ 1 \ 1]. \quad (\text{E31.5})$$

EXERCISE 31.13 [A/C:30]. Derive the consistent and the HRZ-diagonalized lumped mass matrices for a plane stress 10-node cubic triangle with constant mass density ρ and uniform thickness h , moving in the $\{x, y\}$ plane. The triangle has straight sides, side nodes placed at the thirdpoints and node 0 at the centroid. Consequently the metric (and thus the Jacobian) is constant. Show that with the element DOFs arranged $\mathbf{u}^e = [u_{x1} \ u_{y1} \ u_{x2} \ \dots \ u_{y0}]^T$, the CMM is [65, p. 35]

$$\mathbf{M}_C^e = \frac{\rho h A}{6720} \begin{bmatrix} 76 & 0 & 11 & 0 & 11 & 0 & 18 & 0 & 0 & 0 & 27 & 0 & 27 & 0 & 0 & 0 & 18 & 0 & 36 & 0 \\ 0 & 76 & 0 & 11 & 0 & 11 & 0 & 18 & 0 & 0 & 0 & 27 & 0 & 27 & 0 & 0 & 0 & 18 & 0 & 36 \\ 11 & 0 & 76 & 0 & 11 & 0 & 0 & 0 & 18 & 0 & 18 & 0 & 0 & 0 & 27 & 0 & 27 & 0 & 36 & 0 \\ 0 & 11 & 0 & 76 & 0 & 11 & 0 & 0 & 0 & 18 & 0 & 18 & 0 & 0 & 0 & 27 & 0 & 27 & 0 & 36 \\ 11 & 0 & 11 & 0 & 76 & 0 & 27 & 0 & 27 & 0 & 0 & 18 & 0 & 18 & 0 & 0 & 0 & 0 & 36 & 0 \\ 0 & 11 & 0 & 11 & 0 & 76 & 0 & 27 & 0 & 27 & 0 & 0 & 18 & 0 & 18 & 0 & 0 & 0 & 36 & 0 \\ 18 & 0 & 0 & 0 & 27 & 0 & 540 & 0 & -189 & 0 & -135 & 0 & -54 & 0 & -135 & 0 & 270 & 0 & 162 & 0 \\ 0 & 18 & 0 & 0 & 0 & 27 & 0 & 540 & 0 & -189 & 0 & -135 & 0 & -54 & 0 & -135 & 0 & 270 & 0 & 162 \\ 0 & 0 & 18 & 0 & 27 & 0 & -189 & 0 & 540 & 0 & 270 & 0 & -135 & 0 & -54 & 0 & -135 & 0 & 162 & 0 \\ 0 & 0 & 0 & 18 & 0 & 27 & 0 & -189 & 0 & 540 & 0 & 270 & 0 & -135 & 0 & -54 & 0 & -135 & 0 & 162 \\ 27 & 0 & 18 & 0 & 0 & 0 & -135 & 0 & 270 & 0 & 540 & 0 & -189 & 0 & -135 & 0 & -54 & 0 & 162 & 0 \\ 0 & 27 & 0 & 18 & 0 & 0 & 0 & -135 & 0 & 270 & 0 & 540 & 0 & -189 & 0 & -135 & 0 & -54 & 0 & 162 \\ 27 & 0 & 0 & 0 & 18 & 0 & -54 & 0 & -135 & 0 & -189 & 0 & 540 & 0 & 270 & 0 & -135 & 0 & 162 & 0 \\ 0 & 27 & 0 & 0 & 0 & 18 & 0 & -54 & 0 & -135 & 0 & -189 & 0 & 540 & 0 & 270 & 0 & -135 & 0 & 162 \\ 0 & 0 & 27 & 0 & 18 & 0 & -135 & 0 & -54 & 0 & -135 & 0 & 270 & 0 & 540 & 0 & -189 & 0 & 162 & 0 \\ 0 & 0 & 0 & 27 & 0 & 18 & 0 & -135 & 0 & -54 & 0 & -135 & 0 & 270 & 0 & 540 & 0 & -189 & 0 & 162 \\ 18 & 0 & 27 & 0 & 0 & 0 & 270 & 0 & -135 & 0 & -54 & 0 & -135 & 0 & -189 & 0 & 540 & 0 & 162 & 0 \\ 0 & 18 & 0 & 27 & 0 & 0 & 0 & 270 & 0 & -135 & 0 & -54 & 0 & -135 & 0 & -189 & 0 & 540 & 0 & 162 \\ 36 & 0 & 36 & 0 & 36 & 0 & 162 & 0 & 162 & 0 & 162 & 0 & 162 & 0 & 162 & 0 & 162 & 0 & 1944 & 0 \\ 0 & 36 & 0 & 36 & 0 & 36 & 0 & 162 & 0 & 162 & 0 & 162 & 0 & 162 & 0 & 162 & 0 & 162 & 0 & 1944 \end{bmatrix} \quad (\text{E31.6})$$

```

Quad8IsoMembraneConsMass[ncoor_,rho_,h_,{numer_,p_}]:=
Module[{i,k,Nf,dNx,dNy,Jdet,Nfxy,qcoor,w,Me=Table[0,{16},{16}]},
  For [k=1, k<=p*p, k++,
    {qcoor,w}= QuadGaussRuleInfo[{p,numer},k];
    {Nf,dNx,dNy,Jdet}= Quad8IsoPShapeFunDer[ncoor,qcoor];
    Nfxy={Flatten[Table[{Nf[[i]],
                        0},{i,8}]],
          Flatten[Table[{
                        0,Nf[[i]]},{i,8}]]};
    Me+=(rho*w*Jdet*h/2)*Transpose[Nfxy].Nfxy;
  ]; If[!numer,Me=Simplify[Me]]; Return[Me]
];
    
```

FIGURE E31.1. CMM module for 8-node serendipity quadrilateral in plane stress.

Check that all eigenvalues are positive. Show that the HRZ-diagonalized LMM is

$$\mathbf{M}_L^e = \frac{\rho h A}{1353} \text{diag}[19 \ 19 \ 19 \ 19 \ 19 \ 19 \ 135 \ 135 \ 135 \ 135 \ 135 \ 135 \ 135 \ 135 \ 135 \ 135 \ 486 \ 486]. \tag{E31.7}$$

EXERCISE 31.14 [A/C:20]. Derive the consistent mass for a plane stress 4-node bilinear rectangle with constant mass density ρ , uniform thickness h and side dimensions a and b .

EXERCISE 31.15 [A:15]. Explain why, for a plane stress element moving in the $\{x, y\}$ plane, each Gauss integration point adds 2 to the rank of the CMM. What would happen in three dimensions?

EXERCISE 31.16 [A:25]. For *any* geometry, the CMM of the 4-node bilinear quadrilateral in plane stress (assumed homogeneous and of constant thickness) repeats once the $p \times p$ Gauss integration rule verifies $p \geq 2$. Explain why.

EXERCISE 31.17 [C:15]. Using the script of Figure E31.1 derive the consistent and HRZ-diagonalized lumped mass matrices for a 8-node serendipity quadrilateral specialized to a rectangle of dimensions $\{a, b\}$ that moves in the $\{x, y\}$ plane. Assume constant mass density ρ and uniform thickness h . Show that

$$\mathbf{M}_C^e = \frac{\rho abh}{360} \begin{bmatrix} 6 & 0 & 2 & 0 & 3 & 0 & 2 & 0 & -6 & 0 & -8 & 0 & -8 & 0 & -6 & 0 \\ 0 & 6 & 0 & 2 & 0 & 3 & 0 & 2 & 0 & -6 & 0 & -8 & 0 & -8 & 0 & -6 \\ 2 & 0 & 6 & 0 & 2 & 0 & 3 & 0 & -6 & 0 & -6 & 0 & -8 & 0 & -8 & 0 \\ 0 & 2 & 0 & 6 & 0 & 2 & 0 & 3 & 0 & -6 & 0 & -6 & 0 & -8 & 0 & -8 \\ 3 & 0 & 2 & 0 & 6 & 0 & 2 & 0 & -8 & 0 & -6 & 0 & -6 & 0 & -8 & 0 \\ 0 & 3 & 0 & 2 & 0 & 6 & 0 & 2 & 0 & -8 & 0 & -6 & 0 & -6 & 0 & -8 \\ 2 & 0 & 3 & 0 & 2 & 0 & 6 & 0 & -8 & 0 & -8 & 0 & -6 & 0 & -6 & 0 \\ 0 & 2 & 0 & 3 & 0 & 2 & 0 & 6 & 0 & -8 & 0 & -8 & 0 & -6 & 0 & -6 \\ -6 & 0 & -6 & 0 & -8 & 0 & -8 & 0 & 32 & 0 & 20 & 0 & 16 & 0 & 20 & 0 \\ 0 & -6 & 0 & -6 & 0 & -8 & 0 & -8 & 0 & 32 & 0 & 20 & 0 & 16 & 0 & 20 \\ -8 & 0 & -6 & 0 & -6 & 0 & -8 & 0 & 20 & 0 & 32 & 0 & 20 & 0 & 16 & 0 \\ 0 & -8 & 0 & -6 & 0 & -6 & 0 & -8 & 0 & 20 & 0 & 32 & 0 & 20 & 0 & 16 \\ -8 & 0 & -8 & 0 & -6 & 0 & -6 & 0 & 16 & 0 & 20 & 0 & 32 & 0 & 20 & 0 \\ 0 & -8 & 0 & -8 & 0 & -6 & 0 & -6 & 0 & 16 & 0 & 20 & 0 & 32 & 0 & 20 \\ -6 & 0 & -8 & 0 & -8 & 0 & -6 & 0 & 20 & 0 & 16 & 0 & 20 & 0 & 32 & 0 \\ 0 & -6 & 0 & -8 & 0 & -8 & 0 & -6 & 0 & 20 & 0 & 16 & 0 & 20 & 0 & 32 \end{bmatrix} \tag{E31.8}$$

Which is the minimum integration rule required to get this matrix? Show that HRZ gives

$$\mathbf{M}_L^e = \frac{\rho abh}{76} \text{diag}[3 \ 3 \ 3 \ 3 \ 3 \ 3 \ 3 \ 3 \ 16 \ 16 \ 16 \ 16 \ 16 \ 16 \ 16 \ 16]. \tag{E31.9}$$

```

Quad9IsoPMembraneConsMass[ncoor_, ρ_, h_, {numer_, p_}] :=
Module[{i, k, Nf, dNx, dNy, Jdet, Nfxy, qcoor, w, Me=Table[0, {18}, {18}]},
  For [k=1, k<=p*p, k++,
    {qcoor, w}= QuadGaussRuleInfo[{p, numer}, k];
    {Nf, dNx, dNy, Jdet}= Quad9IsoPShapeFunDer[ncoor, qcoor];
    Nfxy={Flatten[Table[{Nf[[i]], 0}, {i, 9}]],
          Flatten[Table[{0, Nf[[i]]}, {i, 9}]]};
    Me+=(ρ*w*Jdet*h/2)*Transpose[Nfxy].Nfxy;
  ]; If[!numer, Me=Simplify[Me]]; Return[Me]
];

```

FIGURE E31.2. CMM module for 9-node biquadratic quadrilateral in plane stress.

EXERCISE 31.18 [C:15]. Using the script of Figure E31.2 derive the consistent and HRZ-diagonalized lumped mass matrices for a 9-node biquadratic quadrilateral specialized to a rectangle of dimensions $\{a, b\}$ that moves in the $\{x, y\}$ plane. Assume constant mass density ρ and uniform thickness h . Show that

$$\mathbf{M}_C^e = \frac{\rho abh}{1800} \begin{bmatrix}
16 & 0 & -4 & 0 & 1 & 0 & -4 & 0 & 8 & 0 & -2 & 0 & -2 & 0 & 8 & 0 & 4 & 0 \\
0 & 16 & 0 & -4 & 0 & 1 & 0 & -4 & 0 & 8 & 0 & -2 & 0 & -2 & 0 & 8 & 0 & 4 \\
-4 & 0 & 16 & 0 & -4 & 0 & 1 & 0 & 8 & 0 & 8 & 0 & -2 & 0 & -2 & 0 & 4 & 0 \\
0 & -4 & 0 & 16 & 0 & -4 & 0 & 1 & 0 & 8 & 0 & 8 & 0 & -2 & 0 & -2 & 0 & 4 \\
1 & 0 & -4 & 0 & 16 & 0 & -4 & 0 & -2 & 0 & 8 & 0 & 8 & 0 & -2 & 0 & 4 & 0 \\
0 & 1 & 0 & -4 & 0 & 16 & 0 & -4 & 0 & -2 & 0 & 8 & 0 & 8 & 0 & -2 & 0 & 4 \\
-4 & 0 & 1 & 0 & -4 & 0 & 16 & 0 & -2 & 0 & -2 & 0 & 8 & 0 & 8 & 0 & 4 & 0 \\
0 & -4 & 0 & 1 & 0 & -4 & 0 & 16 & 0 & -2 & 0 & -2 & 0 & 8 & 0 & 8 & 0 & 4 \\
8 & 0 & 8 & 0 & -2 & 0 & -2 & 0 & 64 & 0 & 4 & 0 & -16 & 0 & 4 & 0 & 32 & 0 \\
0 & 8 & 0 & 8 & 0 & -2 & 0 & -2 & 0 & 64 & 0 & 4 & 0 & -16 & 0 & 4 & 0 & 32 \\
-2 & 0 & 8 & 0 & 8 & 0 & -2 & 0 & 4 & 0 & 64 & 0 & 4 & 0 & -16 & 0 & 32 & 0 \\
0 & -2 & 0 & 8 & 0 & 8 & 0 & -2 & 0 & 4 & 0 & 64 & 0 & 4 & 0 & -16 & 0 & 32 \\
-2 & 0 & -2 & 0 & 8 & 0 & 8 & 0 & -16 & 0 & 4 & 0 & 64 & 0 & 4 & 0 & 32 & 0 \\
0 & -2 & 0 & -2 & 0 & 8 & 0 & 8 & 0 & -16 & 0 & 4 & 0 & 64 & 0 & 4 & 0 & 32 \\
8 & 0 & -2 & 0 & -2 & 0 & 8 & 0 & 4 & 0 & -16 & 0 & 4 & 0 & 64 & 0 & 32 & 0 \\
0 & 8 & 0 & -2 & 0 & -2 & 0 & 8 & 0 & 4 & 0 & -16 & 0 & 4 & 0 & 64 & 0 & 32 \\
4 & 0 & 4 & 0 & 4 & 0 & 4 & 0 & 32 & 0 & 32 & 0 & 32 & 0 & 32 & 0 & 256 & 0 \\
0 & 4 & 0 & 4 & 0 & 4 & 0 & 4 & 0 & 32 & 0 & 32 & 0 & 32 & 0 & 32 & 0 & 256
\end{bmatrix} \quad (\text{E31.10})$$

Which is the minimum integration rule required to get this matrix? Show that HRZ gives

$$\mathbf{M}_L^e = \frac{\rho abh}{36} \mathbf{diag}[1 \ 1 \ 1 \ 1 \ 1 \ 1 \ 1 \ 1 \ 4 \ 4 \ 4 \ 4 \ 4 \ 4 \ 4 \ 4 \ 16 \ 16]. \quad (\text{E31.11})$$

EXERCISE 31.19 A:25] Two Lobatto formulas that may be used for the 9-node biquadratic quadrilateral may be found listed in [227, p. 244–245]. Translated to a rectangle geometry of area A and FEM quadrilateral-coordinate notation, they are

$$\begin{aligned}
\frac{1}{A} \int_{\Omega^e} f(\xi, \eta) d\Omega &= \frac{16}{36} f(0, 0) + \frac{4}{36} [f(0, -1) + f(1, 0) + f(0, 1) + f(-1, 0)] \\
&\quad + \frac{1}{36} [f(-1, -1) + f(1, -1) + f(1, 1) + f(-1, 1)], \quad (\text{E31.12})
\end{aligned}$$

$$\begin{aligned}
\frac{1}{A} \int_{\Omega^e} f(\xi, \eta) d\Omega &= \frac{20}{48} f(0, 0) + \frac{6}{48} [f(0, -1) + f(1, 0) + f(0, 1) + f(-1, 0)] \\
&\quad + \frac{1}{48} [f(-1, -1) + f(1, -1) + f(1, 1) + f(-1, 1)]. \quad (\text{E31.13})
\end{aligned}$$

(E31.12) is a product Simpson formula, whereas (E31.13) was derived by Albrecht and Collatz in 1953. Explain (i) how these formulas can be used to set up a DLMM for a quadrilateral of arbitrary geometry, and (ii) whether (E31.12) coalesces with the HRZ result in the case of a rectangle.